

RSC Advances



This is an *Accepted Manuscript*, which has been through the Royal Society of Chemistry peer review process and has been accepted for publication.

Accepted Manuscripts are published online shortly after acceptance, before technical editing, formatting and proof reading. Using this free service, authors can make their results available to the community, in citable form, before we publish the edited article. This *Accepted Manuscript* will be replaced by the edited, formatted and paginated article as soon as this is available.

You can find more information about *Accepted Manuscripts* in the [Information for Authors](#).

Please note that technical editing may introduce minor changes to the text and/or graphics, which may alter content. The journal's standard [Terms & Conditions](#) and the [Ethical guidelines](#) still apply. In no event shall the Royal Society of Chemistry be held responsible for any errors or omissions in this *Accepted Manuscript* or any consequences arising from the use of any information it contains.

Making A Better Organic-Inorganic Composite Electrolyte to Enhance Cycle Life of Lithium-Sulfur Batteries

Il Young Choi¹, Hoon Kim², and Moon Jeong Park^{1,2*}

¹Division of Advanced Materials Science, ²Department of Chemistry, Pohang University of Science and Technology (POSTECH), Pohang, Korea 790-784

* Corresponding author
(moonpark@postech.edu)

Abstract

A new methodology for resolving the long-standing obstacles of Li-S batteries by the synthesis of a composite gel polymer electrolyte with a unique internal structure is disclosed in this paper. The Li-S cells prepared using this novel electrolyte system exhibit high discharge capacities (1140 mAh/g during the 1st cycle and reversible capacity of 970 mAh/g at the 100th cycle) and improved cycle life.

Considerable efforts have been devoted toward the development of lithium ion batteries (LIBs) for over two decades.¹ In particular, much of the recent work has been devoted to exploiting high-energy density LIBs, with focus on designing new electrode active materials suitable for various applications ranging from mobile phones to large-scale energy storage systems.² Elemental sulfur is one of the most attractive cathode active materials for large-scale energy storage systems by taking advantages of extraordinarily high theoretical specific capacity (1675 mAh/g) and energy density (2567 Wh/kg).³ Further, sulfur presents benefits such as non-toxicity, low price, and natural abundance.

Despite their positive aspects, lithium-sulfur (Li-S) batteries suffer from severe capacity fading during cycling, which is mainly attributed to the dissolution of lithium polysulfide intermediates into liquid electrolytes.⁴ It is likely that the dissolved polysulfides deposit as insoluble solid layers at the electrode surfaces during repeated charge/discharge cycles, leading to an increase in the impedance of the cell, decrease in the Coulombic efficiency, and the loss of active materials.⁵

In this context, many studies have been carried out to overcome the issue of polysulfide dissolution. The most significant progress has been made by employing nanostructured carbon materials as cathode frameworks, which physically encapsulate the sulfur.^{3,6} This approach has been proven to substantially improve the cycle life of Li-S batteries over a few hundred cycles. Of the various strategies, another promising means for inhibiting polysulfide dissolution is by designing a new electrolyte. In particular, polymer electrolytes that can serve as a physical barrier to the diffusion of dissolved polysulfide intermediates from the cathode to the anode are promising.⁷ Mechanical stability and ease of processing, along with flexible form factors, are some additional benefits of the polymer electrolytes. However, these electrolytes have received relatively less attention compared to the cathode materials.

The most widely studied polymer electrolytes can be categorized into solid polymer electrolytes (SPEs)⁸ and gel polymer electrolytes (GPEs).⁹ Poly (ethylene oxide) (PEO)-based polymers have long been considered to be promising candidates for SPEs.¹⁰ However,

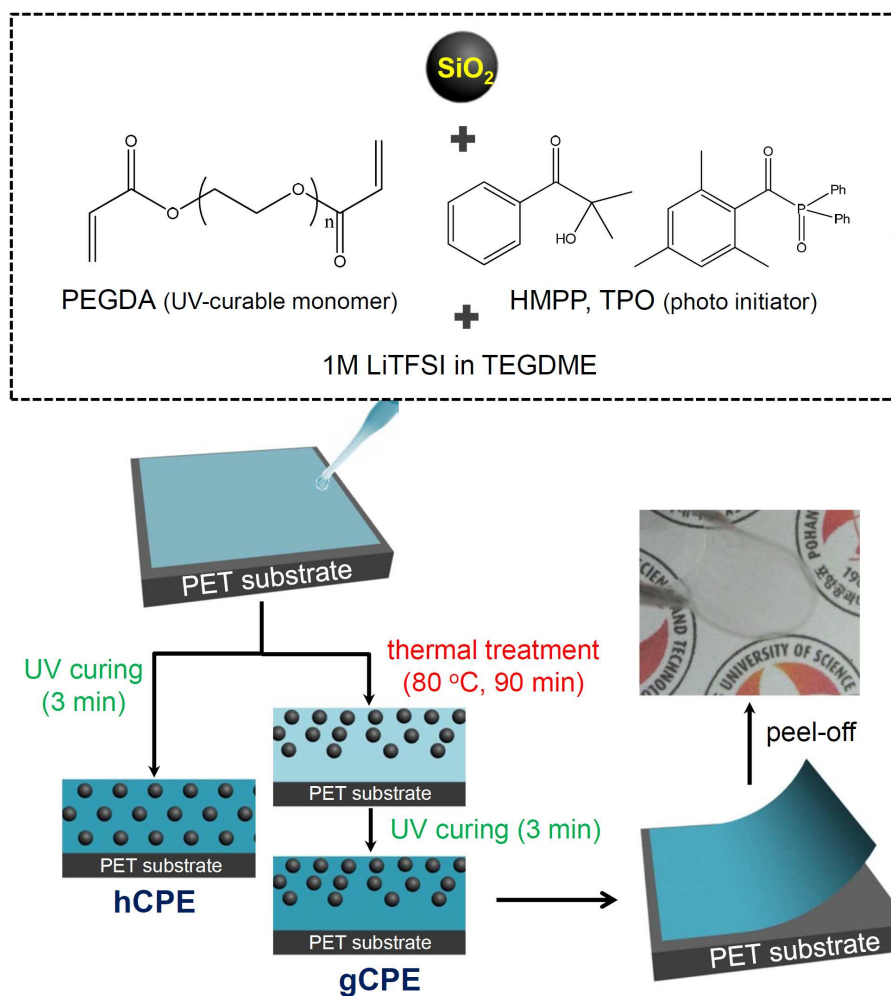
their significantly low ionic conductivity at room temperature ($< 10^{-5}$ S/cm) has been a deterrent to their practical use in batteries. As an alternative for SPEs, GPEs composed of liquid electrolytes with high ionic conductivity embedded within mechanically robust polymer matrices have attracted attention.¹¹ Nevertheless, the application of GPEs in Li-S batteries appears far-fetched, given that long-term battery performance over hundred cycles has been rarely reported. The poor long-term performance is attributed to the dissolution of lithium polysulfides into the GPEs through liquid ingredients.¹²

From this standpoint, the fabrication of composite gel polymer electrolytes (CPEs) by incorporating nanosized inorganic fillers into the GPEs is being explored.^{7a,7b,13} The benefits of CPEs over the conventional GPEs in Li-S battery systems are three-fold. First, they impart improved mechanical properties without significant loss of ionic conductivity. Secondly, the shuttling of lithium polysulfide intermediates between the electrodes is suppressed, owing to the presence of physical barriers (inorganic fillers) when the polysulfides reach the liquid electrolytes. Thirdly, improved lithium salt dissociation is achieved, by incorporating high dielectric constant inorganic materials with a large surface area. Although the potential for application of the CPEs in Li-S batteries appears to be immense, the successful development of Li-S batteries containing CPEs with performance surpassing that of conventional Li-S cells based on liquid electrolytes is still in its infancy.

Herein, we report a new design for CPEs with the goal of increasing the energy density and cycle life of Li-S batteries. Free-standing CPEs with ca. 80 μm thickness were prepared by mixing silica nanoparticles (SNPs), polyethylene glycol diacrylate (PEGDA), and lithium salt-doped tetraethylene glycol dimethyl ether (TEGDME), followed by UV curing for 3 min at room temperature. The SNPs showed a mean diameter of 220 nm and carried a high negative charge of -47 mV (Fig. S1 of ESI), offering the capability of impeding polysulfide dissolution into the electrolyte by electrostatic repulsion. The completion of UV curing was confirmed by Fourier transform infrared spectroscopy (Fig. S2 of ESI).

Scheme 1 depicts the fabrication procedure for the CPEs. We found that while a simple UV curing procedure results in the homogeneous distribution of SNPs in cross-linked

PEO matrices (referred to as **hCPE**), a thermal pre-treatment at 80 °C causes the CPE to maintain SNP density gradients in the thickness direction of the CPE (denser at air surfaces, attributed to low surface tension of the SNPs, referred to as **gCPE**). The inset photograph in Scheme 1 shows the transparent and flexible characteristics of the synthesized CPEs.



Scheme 1 Schematic illustration of the fabrication procedure for **hCPE** and **gCPE**.

Cross-sectional morphologies of **hCPE** and **gCPE** were examined by scanning electron microscopy (SEM), which indicated dissimilar SNP distributions (Fig. 1a). Magnified images of three representative cross-sectional areas of **gCPE**, i.e., near air, center, and near substrate, are presented in the insets to demonstrate the position-dependence of the SNP densities, beneath the air-membrane interface. Interestingly, the ionic conductivity of

gCPE is ca. 10% higher than that of **hCPE** (Fig. S3 of ESI), implying that the distribution of SNPs within the CPEs impacts the Li^+ -ion transport efficiency. Therefore, it is inferred that the densely packed, negatively charged surfaces of SNPs provide a more efficient Li^+ -ion diffusion pathway. It is also noted here that the addition of SNPs in GPE resulted in the enhancement of conductivity (the lower conductivity of GPE than those of **gCPE** and **hCPE**, Fig. S3). This indicates that the SNPs in CPEs should not hinder Li^+ -ion conduction path.

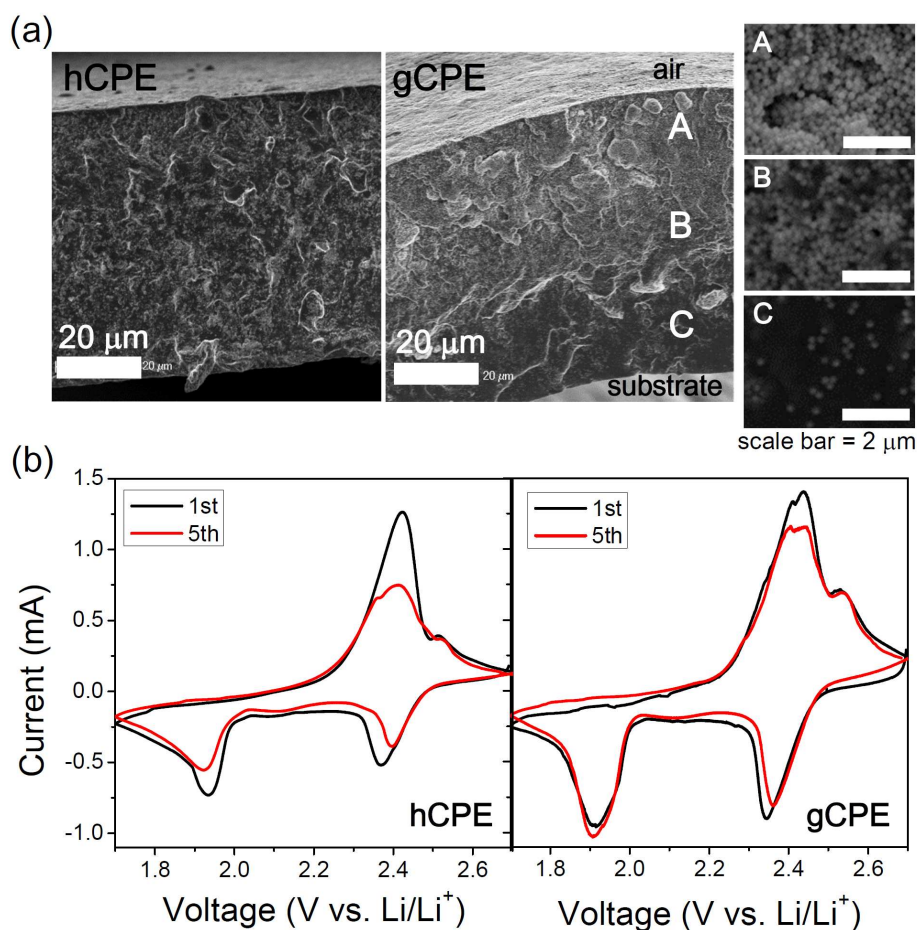


Fig. 1 (a) Cross-sectional SEM images of **hCPE** and **gCPE**. Three representative cross-sectional areas of **gCPE** are magnified in the insets. (b) Cyclic voltammetry of the $\text{Li}/\text{hCPE}/\text{S}$ and $\text{Li}/\text{gCPE}/\text{S}$ cells.

After assembling coin cells containing the **hCPE** and **gCPE** electrolytes, a Li-metal anode, and sulfur in carbon black cathode, the cells were subjected to cyclic voltammetry. (dense SNP side of **gCPE** was placed on the sulfur cathode). Representative data obtained

from the Li/hCPE/S and Li/gCPE/S cells at a scan rate of 0.1 mV s^{-1} are compared in Fig. 1b. Two reduction peaks at 1.9 V and 2.4 V (vs. Li/Li⁺) and one oxidation peak at 2.4 V (and shoulder at 2.5 V) were clearly identified. While shifts in the locations of the reduction peaks and decreases in the peak currents were seen for the Li/hCPE/S cell during subsequent cycles, there were relatively small alterations in the peak locations or currents in the case of the Li/gCPE/S cell as a function of the number of cycles. This indicates the reduced tendency for the formation of a solid electrolyte interface on the cathode as well as intact active materials in the case of gCPE-based cells.

Fig. 2a presents the galvanostatic discharge/charge capacities of the Li/gCPE/S and Li/hCPE/S cells, cycled between 1.7–2.8V at 0.5C, at room temperature. The results of the Li/GPE/S cell, used as control, are also shown. The Li/gCPE/S cell showed an initial discharge capacity of 830 mAh/g (based on the sulfur content), which decreased to 500 mAh/g after 80 cycles with 100% Coulombic efficiency, corresponding to a capacity retention of 60% compared to the initial discharge capacity. This is in sharp contrast with the low discharge capacities and poor capacity retentions seen in the case of the Li/hCPE/S (240 mAh/g, 28%) and Li/GPE/S (133 mAh/g, 20%) cells under the same cycling conditions. The charge/discharge voltage profiles of the three Li-S cells obtained during the first cycle are shown in Fig. 2b, where plateaus at 2.0 V and 2.4 V (vs. Li/Li⁺) during discharging and at 2.4 V during charging were identified.

In the case of the Li/hCPE/S cell, we noticed that most of the capacity fading occurred during the first few cycles, implying a significant loss of active mass into the electrolyte. This result prompted us to elucidate the dependence of the extent of polysulfide dissolution on the CPE structure. The cathode side surface morphologies of gCPE, hCPE, and GPE were examined by SEM equipped with an energy-dispersive X-ray (EDX) spectroscope. The electrolytes were separated from the Li-S cells after five discharge/charge cycles. As shown in Fig. 2c, the surface of gCPE was smooth with an insignificant amount of sulfur aggregates, in contrast with the large sulfur crystals seen for hCPE and GPE. This difference was also clearly seen with the naked eye, as shown in the insets in Fig. 2c. The

amounts of sulfur on the surfaces of **gCPE**, **hCPE**, and GPE determined by EDX were 10, 16, and 27 wt%, respectively, indicating that the polysulfide intermediates are most effectively rendered impermeable by prevalent positioning of negatively charged SNPs near the cathode surfaces. This is likely to be responsible for the improved battery performance seen in the case of the Li/**gCPE**/S cell (Fig. 2a)

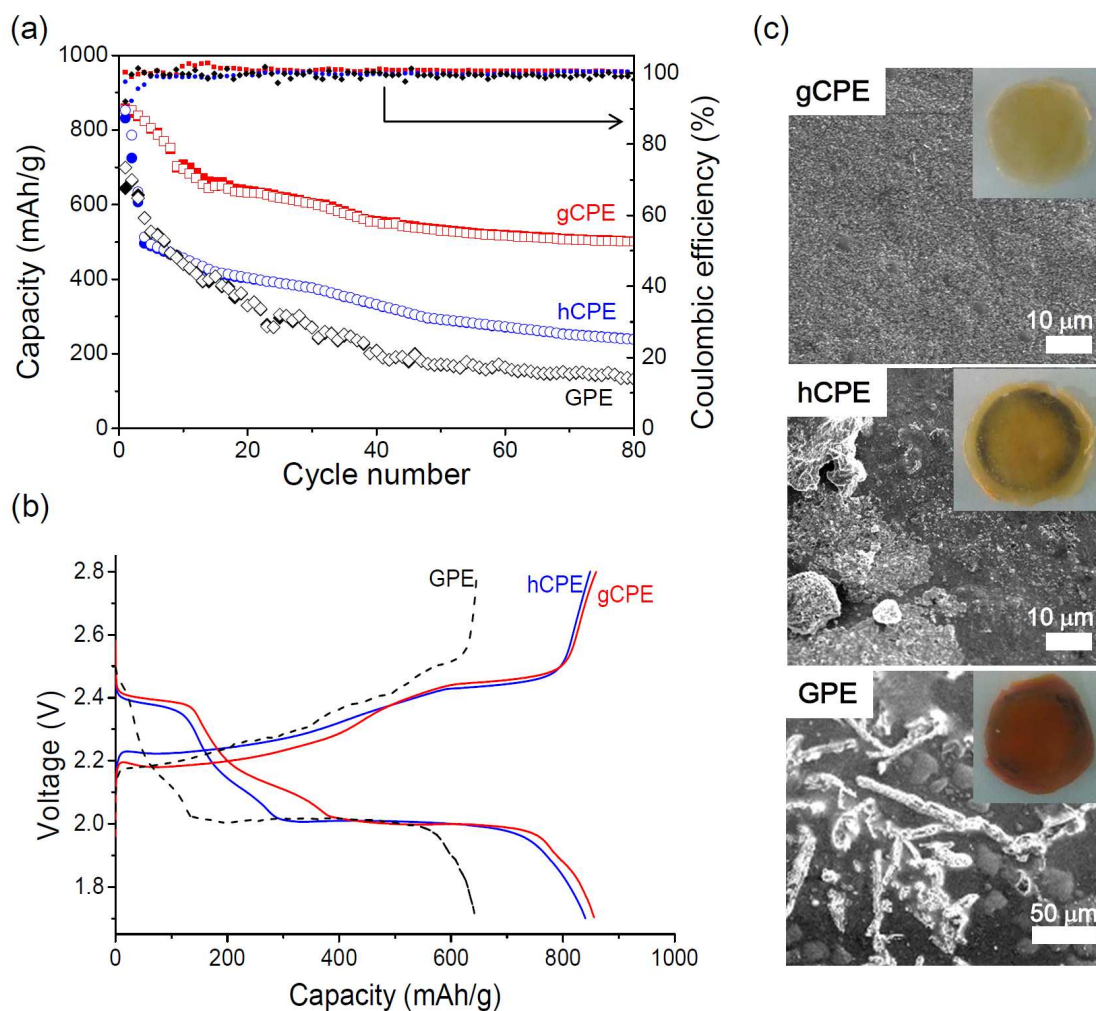


Fig. 2 (a) Galvanostatic discharge/charge capacities of the Li/**gCPE**/S, Li/**hCPE**/S, and Li/GPE/S cells, cycled between 1.7–2.8V at 0.5C at room temperature. (b) The charge/discharge voltage profiles of three Li-S cells obtained for the first cycle. (c) Cathode side surface morphologies of **gCPE**, **hCPE**, and GPE separated from the Li-S cells after five discharge/charge cycles.

It has been proven that the use of optimized sulfur cathodes along with **gCPE** results in Li-S batteries with improved performance. Two types of sulfur cathodes, namely Li_2S in MCMB (S-C) and Li_2S_8 catholyte in gas diffusion layer (S-GDL), were prepared and the discharge/charge cycle properties of the Li/**gCPE**/S-C and Li/**gCPE**/S-GDL cells at 0.2 C rate were examined. As shown in Fig. 3a, an improved cyclability was demonstrated by the Li/**gCPE**/S-C cell, where the battery still maintained a reversible specific discharge capacity of 970 mAh/g after 100 cycles, which is equivalent to 85% capacity retention. In Fig. 3b, representative voltage profiles of the Li/**gCPE**/S-C cell, cycled between 1.9 V and 2.7 V at room temperature are shown. An advanced cycle properties were also observed for the Li/**gCPE**/S-GDL cell, as shown in Fig. 3c. The specific discharge capacity of the Li/**gCPE**/S-GDL cell was 752 mAh/g after 100 cycles, corresponding to capacity retention of 81%. The cell delivered a reversible discharge capacity of 725 mAh/g after 150 cycles (capacity retention of 78%). The results presented above should be significant advances in Li/CPE/S batteries.

In summary, we have proposed a new design for CPEs with the goal of achieving improved Li-S battery cycle life. The exploitation of **gCPE** enabled us to attain a stable discharge capacity of 970mAh/g after 100 cycles. The improved long-term cycle life is believed to be as a result of the strategic positioning of negatively charged SNPs near the cathode surfaces, in order to decelerate the dissolution of polysulfides into the CPE during battery cycling. To the best of our knowledge, this is the first work to unveil the important role played by the internal structure of the CPEs in determining the performance of Li-S cells.

Acknowledgements

This work was financially supported by the Global Frontier R&D program on Center for Multiscale Energy System funded by the National Research Foundation (NRF) of Korea under the Ministry of Education, Science and Technology.

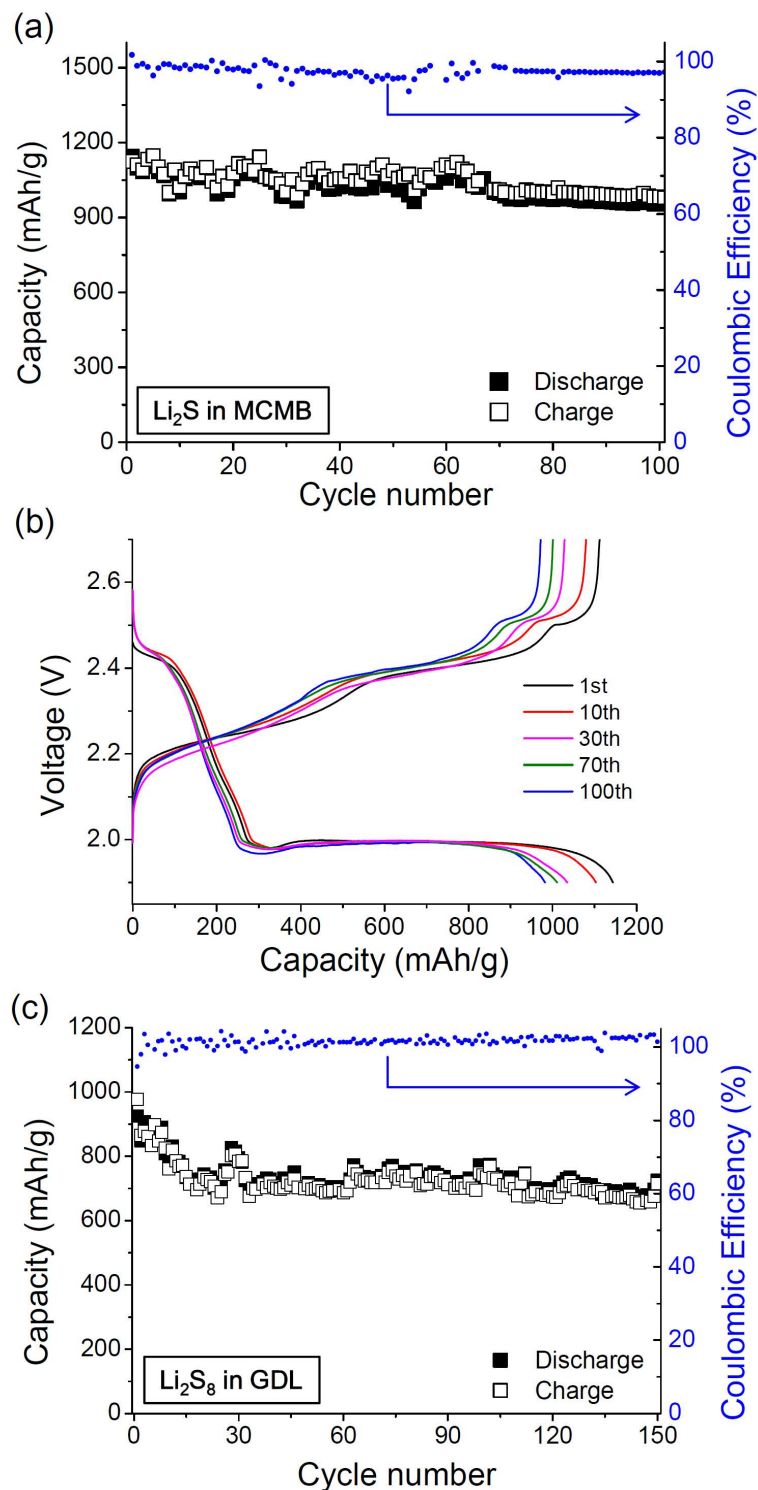


Fig. 3 Galvanostatic discharge/charge capacities of (a) the Li/gCPE/S-GDL and (b) Li/gCPE/S-C cells, cycled between 1.9–2.7V at 0.2C at room temperature. (c) Representative charge/discharge voltage profiles of the Li/gCPE/S-C cells obtained with cycling.

Notes and references

Electronic Supplementary Information (ESI) available: experimental details, SEM & Zetapotential of SNPs, FT-IR of CPEs, ionic conductivities of CPEs and GPE, and Nyquist plots of the Li-S cells. See DOI: 10.1039/c000000x/

1. a) Y. Li, B. Tan and Y. Wu, *Nano Lett.* 2008, **8**, 265-270; b) P. L. Taberna, S. Mitra, P. Poizot, P. Simon and J.-M. Tarascon, *Nat. Mater.*, 2006, **5**, 567-573; c) H. Li, Z. Wang, L. Chen and X. Huang, *Adv. Mater.* 2009, **21**, 4593-4607; d) B. Scrosati, J. Hassounab and Y.-K. Sun, *Energy Environ. Sci.*, 2011, **4**, 3287-3295.
2. a) M. Armand and J.-M. Tarascon, *Nature*, 2008, **451**, 652-657; b) I. Choi, H. Ahn and M. J. Park, *Macromolecules*, 2011, **44**, 7327-7334; c) G. Jo, I. Choi, H. Ahn and M. J. Park, *Chem. Commun.*, 2012, **48**, 3987-3989; d) H. Wang, L.-F. Cui, Y. Yang, H. S. Casalongue, J. T. Robinson, Y. Liang, Y. Cui and H. Dai, *J. Am. Chem. Soc.*, 2010, **132**, 13978-13980; e) B. Kang and G. Ceder, *Nature*, 2009, **458**, 190-193.
3. a) X. Ji, K. T. Lee and L. F. Nazar, *Nat. Mater.*, 2009, **8**, 500-506; b) N. Jayaprakash, J. Shen, S. S. Moganty, A. Corona and L. A. Archer, *Angew. Chem.* 2011, **123**, 6026-6030.
4. a) X. Ji, S. Evers, R. Black and L. F. Nazar, *Nat. Commun.*, 2011, **2**, 325; b) J. Gao, M. A. Lowe, Y. Kiya and H. D. Abruna, *J. Phys. Chem. C.*, 2011, **115**, 25132-25137.
5. a) S. Xin, L. Gu, N.-H. Zhao, Y.-X. Yin, L.-J. Zhou, Y.-G. Guo and L.-J. Wan, *J. Am. Chem. Soc.*, 2012, **134**, 18510-18513; b) S. Evers and L. F. Nazar, *Acc. Chem. Res.*, 2013, **46**, 1135-1143; c) J. Guo, Z. Yang, Y. Yu, H. D. Abruña and L. A. Archer, *J. Am. Chem. Soc.*, 2013, **135**, 763-767.
6. a) G. Zheng, Y. Yang, J. J. Cha, S. S. Hong and Y. Cui, *Nano Lett.*, 2011, **11**, 4462-4467; b) S. Zhao, C. Li, W. Wang, H. Zhang, M. Gao, X. Xiong, A. Wang, K. Yuan, Y. Huang and F. Wang, *J. Mater. Chem. A.*, 2013, **1**, 3334-3339; c) S. Jiang, Z. Zhang, X. Wang, Y. Qu, Y. Lai and J. Li, *RSC Adv.*, 2013, **3**, 16318-16321; d) S. Lu, Y. Chen, X. Wu, Z. Wang, L. Lv, W. Qin and L. Jiang, *RSC Adv.*, 2014, **4**, 18052-18054.
7. a) J. Hassoun and B. Scrosati, *Adv. Mater.* 2010, **22**, 5198-5201; b) K. Jeddi, M. Ghaznavi

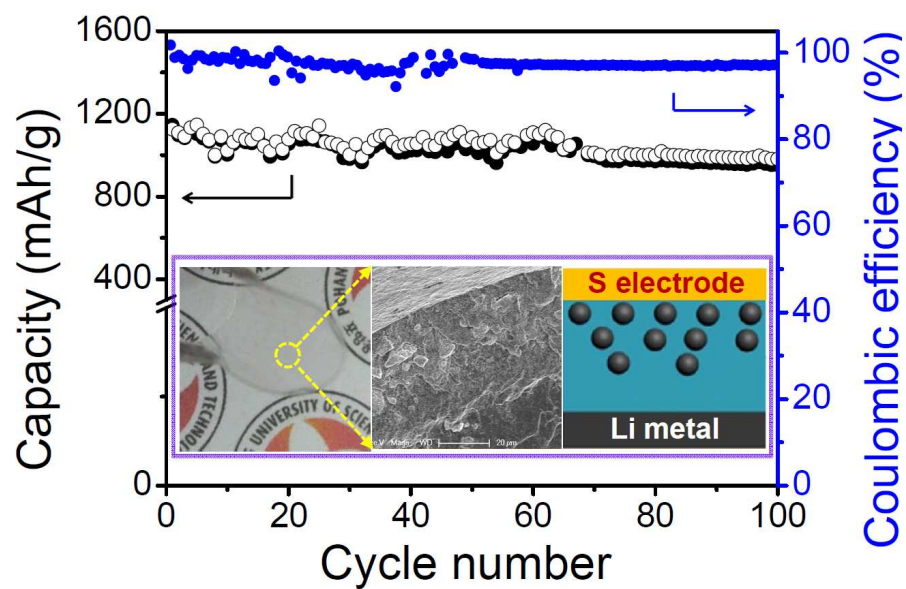
- and P. Chen, *J. Mater. Chem. A.*, 2013, **1**, 2769-2772; c) S. S. Zhang, *J. Electrochem. Soc.*, 2013, **160**, A1421-A1424; d) S. S. Zhang and D. T. Tran, *J. Mater. Chem. A.*, 2014, **2**, 7383-7388; e) Z. Jin, K. Xie and X. Hong, *RSC Adv.*, 2013, **3**, 8889-8898.
8. a) R. C. Agrawal and G. P. Pandey, *J. Phys. D: Appl. Phys.*, 2008, **41**, 223001; b) C. Zhang, S. Gamble, D. Ainsworth, A. M. Z. Slawin, Y. G. Andreev and P. G. Bruce, *Nat. Mater.*, 2009, **8**, 580-584.
9. a) W. Huang, Z. Zhu, L. Wang, S. Wang, H. Li, Z. Tao, J. Shi, L. Guan and J. Chen, *Angew. Chem.* 2013, **125**, 9332-9336; b) J.-H. Park, J.-S. Kim, E.-G. Shim, K.-W. Park, Y. T. Hong, Y.-S. Lee and S.-Y. Lee, *Electrochem. Commun.*, 2010, **12**, 1099-1102.
10. a) J.-H. Shin, W. A. Henderson and S. Passerini, *J. Electrochem. Soc.*, 2005, **152**, A978-A983; b) P. P. Soo, B. Huang, Y.-I. Jang, Y.-M. Chiang, D. R. Sadoway and A. M. Mayes, *J. Electrochem. Soc.*, 1999, **146**, 32-37; c) M. Singh, O. Odusanya, G. M. Wilmes, H. B. Eitouni, E. D. Gomez, A. J. Patel, V. L. Chen, M. J. Park, P. Fragouli, H. Iatrou, N. Hadjichristidis, D. Cookson, N. P. Balsara, *Macromolecules* 2007, **40**, 4578-4585.
11. a) M. Deka and A. Kumar, *Electrochimica Acta*, 2010, **55**, 1836-1842; b) J. R. Nair, C. Gerbaldi, G. Meligrana, R. Bongiovanni, S. Bodoardo, N. Penazzi, P. Reale and V. Gentili, *J. Power Sources*, 2008, **178**, 751-757; c) S. S. Zhang and D. T. Tran, *Electrochimica Acta*, 2013, **114**, 296-302.
12. a) J. Jin, Z. Wen, X. Liang, Y. Cui and X. Wu, *Solid State Ionics*, 2012, **225**, 604-607; b) Z. Jin, K. Xie, X. Hong and Z. Hu, *J. Power Sources*, 2013, **242**, 478-485.
13. a) Y. Zhu, S. Xiao, Y. Shi, Y. Yang, Y. Hou and Y. Wu, *Adv. Energy Mater.* 2014, **4**, 1300647; b) K. Jeddi, Y. Zhao, Y. Zhang, A. Konarov and P. Chen, *J. Electrochem. Soc.*, 2013, **160**, A1052-A1060.

For Table of contents entry use only

Making A Better Organic-Inorganic Composite Electrolyte to Enhance Cycle Life of Lithium-Sulfur Batteries

Il Young Choi¹, Hoon Kim², and Moon Jeong Park^{1,2*}

¹Division of Advanced Materials Science, ²Department of Chemistry, Pohang University of Science and Technology (POSTECH), Pohang, Korea 790-784



The development of high performance Li-S battery based on composite gel polymer electrolyte holding unique density gradients of silica nanoparticles.